

# Synthesis and Structural Characterization of Dinuclear Manganese(III) Complexes with Cyclam-Based Macrocyclic Ligands Having Schiff-Base Pendant Arms as Chelating Agents

Shusaku Wada and Masahiro Mikuriya\*

Department of Chemistry and Open Research Center for Coordination Molecule-based Devices,  
School of Science and Technology, Kwansei Gakuin University, 2-1 Gakuen, Sanda 669-1337

Received October 5, 2007; E-mail: junpei@kwansei.ac.jp

Reaction of a series of dodecadentate ligands ( $H_4L$ ), 1,4,8,11-tetrakis(salicylideneaminoethyl)-1,4,8,11-tetraazacyclotetradecane and its substituted derivatives, with manganese(II) salts afforded ten dinuclear manganese(III) complexes,  $[Mn_2X_2L]$  ( $X = O_2CCH_3$ ,  $O_2CC_6H_5$ , and  $N_3$ ), which were characterized by analyzing infrared and electronic spectra and determining the temperature dependence of magnetic susceptibilities (4.5–300 K). Single-crystal X-ray crystallography of  $[Mn_2(O_2CCH_3)_2(tbsaec)] \cdot 2CHCl_3$  (**3**· $2CHCl_3$ ) ( $H_4tbsaec = 1,4,8,11$ -tetrakis(5-bromosalicylideneaminoethyl)-1,4,8,11-tetraazacyclotetradecane),  $[Mn_2(O_2CC_6H_5)_2(tbsaec)]$  (**4**),  $[Mn_2(O_2CC_6H_5)_2(tcsaec)]$  (**6**) ( $H_4tcsaec = 1,4,8,11$ -tetrakis(5-chlorosalicylideneaminoethyl)-1,4,8,11-tetraazacyclotetradecane),  $[Mn_2(N_3)_2(tnaec)] \cdot 2CHCl_3$  (**7**· $2CHCl_3$ ) ( $H_4tnaec = 1,4,8,11$ -tetrakis(2-hydroxy-1-naphthylmethylideneaminoethyl)-1,4,8,11-tetraazacyclotetradecane),  $[Mn_2(O_2CCH_3)_2(tmsaec)]$  (**8**) ( $H_4tmsaec = 1,4,8,11$ -tetrakis(3-methoxysalicylideneaminoethyl)-1,4,8,11-tetraazacyclotetradecane) showed that each manganese(III) ion is chelated by two Schiff-base pendant arms outside the central tetraazacyclotetradecane ring, forming an axially compressed octahedron (for **3**, **4**, **6**, and **8**) or trigonal bipyramid (for **7**) with an intramolecular Mn–Mn distance of 9.676(4)–10.096(2) Å. In accordance with the crystal structures, the magnetic interaction between the two manganese ions was very weak with a rather significant zero-field splitting of the manganese(III) ions.

There is a continuing interest in the chemistry of metal complexes of tetraazamacrocycles. Introduction of functional pendant arms to tetraazamacrocycles has produced a large number of metal complexes and attracted intensive interest because of their specific structures, chemical properties, and potential applications, such as extraction of metal ions and pharmaceutical and biomedical NMR studies.<sup>1</sup> For example, the thermodynamic stability and kinetic inertness of the 1,4,7,10-tetraazacyclododecane-1,4,7,10-tetraacetate complexes with trivalent metal ions make this pendant-appended macrocyclic ligand one of the most effective and safest contrast agents for magnetic resonance imaging.<sup>1h,2</sup> These types of tetraazamacrocyclic ligands usually bind one metal ion within the macrocyclic cavity forming complexes in a 1:1 molar ratio. Contrary to most tetraazamacrocyclic ligands, an *N*-substituted octadentate ligand derived from 1,4,8,11-tetraazacyclotetradecane (cyclam) having four aminoethyl pendant arms, 1,4,8,11-tetrakis(2-aminoethyl)-1,4,8,11-tetraazacyclotetradecane (taec), exclusively forms dinuclear metal species with various metal ions, such as  $Cr^{II}$ ,  $Co^{II}$ ,  $Ni^{II}$ ,  $Cu^{II}$ ,  $Zn^{II}$ , and  $Cd^{II}$  ions.<sup>3</sup> So far only two types of structures are known for these systems in the solid state: one is a *trans*-III conformation<sup>4</sup> involving a cyclam ring as found in  $[M_2(taec)]X_4$  ( $M = Cr^{II}$ ,  $Ni^{II}$ , and  $Cu^{II}$ ;  $X = ClO_4^-$ ,  $BF_4^-$ , and  $Br^-$ ), and the other is a *trans*-I form<sup>4</sup> as found in anion-bridged complexes of  $[M_2(taec)X]Y_{2or3}$  ( $M = Co^{II}$ ,  $Ni^{II}$ ,  $Cu^{II}$ ,  $Zn^{II}$ , and  $Cd^{II}$ ;  $X = Cl^-$ ,  $Br^-$ ,  $I^-$ ,  $OH^-$ , and  $CO_3^{2-}$ ;  $Y = ClO_4^-$ ,  $PF_6^-$ ,  $CF_3SO_3^-$ ,  $BPh_4^-$ , and  $Cl^-$ ).<sup>3</sup> As for manganese ion, we expected to be able to prepare

dinuclear metal complexes by using this ligand and examined reactions of taec with several manganese salts. However, we could not obtain manganese complexes with taec, possibly because of the low affinity of the pendant amino-nitrogen donors for manganese ions. It is well known that Schiff-base ligands have been often used to construct manganese systems, because the combination of the oxygen and nitrogen donor atoms are favorable for binding manganese ions.<sup>5</sup> For example, tetradentate  $N_2O_2$  Schiff-base salen ligand ( $H_2salen =$  disalicylideneethylenediamine) forms a number of manganese(III) complexes of type  $[Mn(salen)X]$  ( $X =$  monovalent anion).<sup>5a</sup> Many manganese complexes of Schiff-base ligands have been prepared as potential model compounds for the oxygen-evolving complex (OEC) of photosystem II (PSII) in green plants, in which the existence of tetranuclear manganese site in the  $S_0$ – $S_4$  states is widely accepted.<sup>5–11</sup> In this study, we introduced six kinds of salicylideneaminoethyl derivatives in place of the pendant aminoethyl groups of the cyclam ring by using a condensation reaction with salicylaldehyde, four of its commercially available 3-, 5-, and 3,5-substituted derivatives, and 2-hydroxy-1-naphthaldehyde in order to design new Schiff-base ligands and studied the reactivity of these ligands with manganese(II) salts in the hope of obtaining new types of manganese complexes. We report here the synthesis and characterization of dinuclear manganese(III) complexes with these cyclam-based Schiff-base ligands. A preliminary description of one of these complexes has been previously reported.<sup>12</sup>

## Experimental

**Synthesis.** Unless otherwise specified, all reagents were purchased commercially and used without further purification. The parent compound, 1,4,8,11-tetrakis(2-aminoethyl)-1,4,8,11-tetraazacyclotetradecane (taec), was synthesized by a previously reported procedure.<sup>3b</sup>

**1,4,8,11-Tetrakis(5-bromosalicylideneaminoethyl)-1,4,8,11-tetraazacyclotetradecane ( $H_4tbsaec$ ).** Taec (51 mg, 0.14 mmol) was dissolved in methanol (5 cm<sup>3</sup>). To this solution was added 5-bromosalicylaldehyde (111 mg, 0.55 mmol) dissolved in 5 cm<sup>3</sup> of methanol, and the mixture was stirred for 1 h at room temperature. The resulting yellow precipitate was filtered off and washed with methanol. Yield: 105 mg (70%). Anal. Found: C, 49.70; H, 5.18; N, 10.11%. Calcd for C<sub>46</sub>H<sub>56</sub>Br<sub>4</sub>N<sub>8</sub>O<sub>4</sub>·0.5CH<sub>3</sub>OH: C, 49.84; H, 5.22; N, 10.00%. IR (KBr):  $\nu(\text{Ar-H})$  3083,  $\nu_{\text{as}}(\text{CH}_2)$  2970,  $\nu_{\text{s}}(\text{CH}_2)$  2790,  $\nu(\text{C=N})$  1634 cm<sup>-1</sup>. Diffuse reflectance spectrum:  $\lambda_{\text{max}}$  227, 261, 332, 431 nm. UV-vis:  $\lambda_{\text{max}}$  ( $\epsilon/\text{M}^{-1}\text{cm}^{-1}$ , measured in CHCl<sub>3</sub>) 330 (16600), 424 (1300) nm.

**1,4,8,11-Tetrakis(5-chlorosalicylideneaminoethyl)-1,4,8,11-tetraazacyclotetradecane ( $H_4tcsaec$ ).** This ligand was obtained as yellow precipitate by the reaction of taec (52 mg, 0.14 mmol) and 5-chlorosalicylaldehyde (92 mg, 0.59 mmol) in methanol using the same method as that for  $H_4tbsaec$ . Yield: 91 mg (70%). Anal. Found: C, 59.19; H, 6.18; N, 12.09%. Calcd for C<sub>46</sub>H<sub>56</sub>Cl<sub>4</sub>N<sub>8</sub>O<sub>4</sub>·0.5H<sub>2</sub>O: C, 59.04; H, 6.14; N, 11.97%. IR (KBr):  $\nu(\text{Ar-H})$  3088,  $\nu_{\text{as}}(\text{CH}_2)$  2975,  $\nu_{\text{s}}(\text{CH}_2)$  2791,  $\nu(\text{C=N})$  1635 cm<sup>-1</sup>. Diffuse reflectance spectrum:  $\lambda_{\text{max}}$  224, 262, 330, 430 nm. UV-vis:  $\lambda_{\text{max}}$  ( $\epsilon/\text{M}^{-1}\text{cm}^{-1}$ , measured in CHCl<sub>3</sub>) 329 (16900), 424 (1030) nm.

**1,4,8,11-Tetrakis(2-hydroxy-1-naphthylmethylideneaminoethyl)-1,4,8,11-tetraazacyclotetradecane ( $H_4tnaec$ ).** This ligand was obtained as yellow precipitate by the reaction of taec (50 mg, 0.13 mmol) and 2-hydroxy-1-naphthaldehyde (96 mg, 0.56 mmol) in methanol using the same method as that for  $H_4tbsaec$ . Yield: 103 mg (77%). Anal. Found: C, 70.66; H, 7.14; N, 10.54%. Calcd for C<sub>62</sub>H<sub>68</sub>N<sub>8</sub>O<sub>4</sub>·0.5CH<sub>3</sub>OH·3H<sub>2</sub>O: C, 70.86; H, 7.23; N, 10.58%. IR (KBr):  $\nu(\text{Ar-H})$  3061,  $\nu_{\text{as}}(\text{CH}_2)$  2938,  $\nu_{\text{s}}(\text{CH}_2)$  2807,  $\nu(\text{C=N})$  1630 cm<sup>-1</sup>. Diffuse reflectance spectrum:  $\lambda_{\text{max}}$  225, 274, 307, 387, 424 nm. UV-vis:  $\lambda_{\text{max}}$  ( $\epsilon/\text{M}^{-1}\text{cm}^{-1}$ , measured in CHCl<sub>3</sub>) 264 (51900), 274sh (35900), 310 (38300), 404 (32700), 422 (33700) nm.

**[Mn<sub>2</sub>(O<sub>2</sub>CCH<sub>3</sub>)<sub>2</sub>(tsaec)] (1).** A methanol solution (2 cm<sup>3</sup>) of salicylaldehyde (39 mg, 0.32 mmol) was added dropwise to a stirred solution of taec (30 mg, 0.08 mmol) in methanol (5 cm<sup>3</sup>) at room temperature. To this solution was added a methanol solution (7 cm<sup>3</sup>) of manganese(II) acetate tetrahydrate (40 mg, 0.16 mmol). The reaction mixture was allowed to stand at room temperature, affording dark brown crystals. Yield: 46 mg (56%). Anal. Found: C, 59.49; H, 6.19; N, 10.89%. Calcd for C<sub>50</sub>H<sub>62</sub>Mn<sub>2</sub>N<sub>8</sub>O<sub>8</sub>: C, 59.29; H, 6.17; N, 11.06%. IR (KBr):  $\nu(\text{Ar-H})$  3052,  $\nu_{\text{as}}(\text{CH}_2)$  2984,  $\nu_{\text{s}}(\text{CH}_2)$  2792,  $\nu(\text{C=N})$  1620,  $\nu_{\text{as}}(\text{CO}_2^-)$  1551,  $\nu_{\text{s}}(\text{CO}_2^-)$  1447 cm<sup>-1</sup>. Diffuse reflectance spectrum:  $\lambda_{\text{max}}$  227, 262, 360, 527br, 706 nm.

**[Mn<sub>2</sub>(O<sub>2</sub>CC<sub>6</sub>H<sub>5</sub>)<sub>2</sub>(tsaec)] (2).** The complex was prepared in the same way as **1**, except that manganese(II) benzoate dihydrate was used instead of manganese(II) acetate tetrahydrate. Yield: 51 mg (58%). Anal. Found: C, 63.20; H, 5.87; N, 9.73%. Calcd for C<sub>60</sub>H<sub>66</sub>Mn<sub>2</sub>N<sub>8</sub>O<sub>8</sub>: C, 63.38; H, 5.85; N, 9.85%. IR (KBr):  $\nu(\text{Ar-H})$  3049,  $\nu_{\text{as}}(\text{CH}_2)$  2981,  $\nu_{\text{s}}(\text{CH}_2)$  2791,  $\nu(\text{C=N})$  1625,  $\nu_{\text{as}}(\text{CO}_2^-)$  1548,  $\nu_{\text{s}}(\text{CO}_2^-)$  1445 cm<sup>-1</sup>. Diffuse reflectance spectrum:  $\lambda_{\text{max}}$  226, 263sh, 365, 438br, 705 nm.

**[Mn<sub>2</sub>(O<sub>2</sub>CCH<sub>3</sub>)<sub>2</sub>(tbsaec)]·2CHCl<sub>3</sub>·CH<sub>3</sub>OH (3·2CHCl<sub>3</sub>·**

**CH<sub>3</sub>OH).**  $H_4tbsaec$  (33 mg, 0.03 mmol) was dissolved in CHCl<sub>3</sub> (5 cm<sup>3</sup>). To this solution was added a methanol solution (10 cm<sup>3</sup>) of manganese(II) acetate tetrahydrate (15 mg, 0.06 mmol). The reaction mixture was allowed to stand at room temperature, which gave dark brown crystals. Yield: 34 mg (70%). Anal. Found: C, 40.09; H, 4.18; N, 7.14%. Calcd for C<sub>50</sub>H<sub>58</sub>Br<sub>4</sub>Mn<sub>2</sub>N<sub>8</sub>O<sub>8</sub>·2CHCl<sub>3</sub>·CH<sub>3</sub>OH: C, 39.80; H, 4.03; N, 7.01%. IR (KBr):  $\nu_{\text{as}}(\text{CH}_2)$  2983,  $\nu_{\text{s}}(\text{CH}_2)$  2803,  $\nu(\text{C=N})$  1618,  $\nu_{\text{as}}(\text{CO}_2^-)$  1556,  $\nu_{\text{s}}(\text{CO}_2^-)$  1458 cm<sup>-1</sup>. Diffuse reflectance spectrum:  $\lambda_{\text{max}}$  255br, 370, 453sh, 720 nm.

**[Mn<sub>2</sub>(O<sub>2</sub>CC<sub>6</sub>H<sub>5</sub>)<sub>2</sub>(tbsaec)]·0.5CHCl<sub>3</sub>·H<sub>2</sub>O (4·0.5CHCl<sub>3</sub>·H<sub>2</sub>O).** The complex was prepared in the same way as **3**, except that manganese(II) benzoate dihydrate was used instead of manganese(II) acetate tetrahydrate. Yield: 28 mg (62%). Anal. Found: C, 47.31; H, 4.62; N, 7.34%. Calcd for C<sub>60</sub>H<sub>62</sub>Br<sub>4</sub>Mn<sub>2</sub>N<sub>8</sub>O<sub>8</sub>·0.5CHCl<sub>3</sub>·H<sub>2</sub>O: C, 47.48; H, 4.25; N, 7.32%. IR (KBr):  $\nu(\text{Ar-H})$  3050,  $\nu_{\text{as}}(\text{CH}_2)$  2979,  $\nu_{\text{s}}(\text{CH}_2)$  2792,  $\nu(\text{C=N})$  1623,  $\nu_{\text{as}}(\text{CO}_2^-)$  1536,  $\nu_{\text{s}}(\text{CO}_2^-)$  1454 cm<sup>-1</sup>. Diffuse reflectance spectrum:  $\lambda_{\text{max}}$  228, 265sh, 368, 446sh, 707 nm.

**[Mn<sub>2</sub>(O<sub>2</sub>CCH<sub>3</sub>)<sub>2</sub>(tcsaec)]·2H<sub>2</sub>O (5·2H<sub>2</sub>O).** The complex was prepared in the same way as **3**, except that  $H_4tcsaec$  was used instead of  $H_4tbsaec$ . Yield: 25 mg (71%). Anal. Found: C, 50.86; H, 5.30; N, 9.37%. Calcd for C<sub>50</sub>H<sub>58</sub>Cl<sub>4</sub>Mn<sub>2</sub>N<sub>8</sub>O<sub>8</sub>·2H<sub>2</sub>O: C, 50.60; H, 5.27; N, 9.44%. IR (KBr):  $\nu_{\text{as}}(\text{CH}_2)$  2984,  $\nu_{\text{s}}(\text{CH}_2)$  2792,  $\nu(\text{C=N})$  1620,  $\nu_{\text{as}}(\text{CO}_2^-)$  1561,  $\nu_{\text{s}}(\text{CO}_2^-)$  1461 cm<sup>-1</sup>. Diffuse reflectance spectrum:  $\lambda_{\text{max}}$  236, 371, 453sh, 540br, 715 nm.

**[Mn<sub>2</sub>(O<sub>2</sub>CC<sub>6</sub>H<sub>5</sub>)<sub>2</sub>(tcsaec)]·2H<sub>2</sub>O (6·2H<sub>2</sub>O).** The complex was prepared in the same way as **5**, except that manganese(II) benzoate dihydrate was used instead of manganese(II) acetate tetrahydrate. Yield: 22 mg (57%). Anal. Found: C, 54.74; H, 5.30; N, 8.66%. Calcd for C<sub>60</sub>H<sub>62</sub>Cl<sub>4</sub>Mn<sub>2</sub>N<sub>8</sub>O<sub>8</sub>·2H<sub>2</sub>O: C, 54.97; H, 5.08; N, 8.55%. IR (KBr):  $\nu(\text{Ar-H})$  3058,  $\nu_{\text{as}}(\text{CH}_2)$  2983,  $\nu_{\text{s}}(\text{CH}_2)$  2790,  $\nu(\text{C=N})$  1624,  $\nu_{\text{as}}(\text{CO}_2^-)$  1542,  $\nu_{\text{s}}(\text{CO}_2^-)$  1457 cm<sup>-1</sup>. Diffuse reflectance spectrum:  $\lambda_{\text{max}}$  228, 257sh, 374, 454sh, 709 nm.

**[Mn<sub>2</sub>(N<sub>3</sub>)<sub>2</sub>(tnaec)]·2CHCl<sub>3</sub>·2CH<sub>3</sub>OH (7·2CHCl<sub>3</sub>·2CH<sub>3</sub>·OH).**  $H_4tnaec$  (30 mg, 0.03 mmol) was dissolved in CHCl<sub>3</sub> (7 cm<sup>3</sup>). To this solution were added a methanol solution (7 cm<sup>3</sup>) of manganese(II) acetate tetrahydrate (15 mg, 0.06 mmol) and an aqueous solution (0.1 cm<sup>3</sup>) of sodium azide (8 mg, 0.12 mmol). The mixture was allowed to stand at room temperature to give dark brown crystals. Yield: 27 mg (61%). Anal. Found: C, 53.22; H, 4.97; N, 13.06%. Calcd for C<sub>62</sub>H<sub>64</sub>Mn<sub>2</sub>N<sub>14</sub>O<sub>4</sub>·2CHCl<sub>3</sub>·2CH<sub>3</sub>·OH: C, 53.49; H, 5.03; N, 13.23%. IR (KBr):  $\nu(\text{Ar-H})$  3000,  $\nu_{\text{as}}(\text{CH}_2)$  2933,  $\nu_{\text{s}}(\text{CH}_2)$  2797,  $\nu(\text{N}_3)$  2038,  $\nu(\text{C=N})$  1616 cm<sup>-1</sup>. Diffuse reflectance spectrum:  $\lambda_{\text{max}}$  241, 336, 428, 688 nm. UV-vis:  $\lambda_{\text{max}}$  ( $\epsilon/\text{M}^{-1}\text{cm}^{-1}$ , measured in DMSO) 308 (34900), 330sh (31600), 402 (16100), 422 (14700), 625 (868) nm.

**[Mn<sub>2</sub>(O<sub>2</sub>CCH<sub>3</sub>)<sub>2</sub>(tmsaec)]·3H<sub>2</sub>O (8·3H<sub>2</sub>O).** To an acetonitrile solution (15 cm<sup>3</sup>) of taec (31 mg, 0.08 mmol) were added 3-methoxysalicylaldehyde (51 mg, 0.33 mmol) and manganese(II) acetate tetrahydrate (63 mg, 0.26 mmol). The mixture was heated for 5 min at 60 °C. The resulting dark brown solution was allowed to stand at room temperature to give dark brown crystals. Yield: 46 mg (48%). Anal. Found: C, 54.79; H, 5.98; N, 9.48%. Calcd for C<sub>54</sub>H<sub>70</sub>Mn<sub>2</sub>N<sub>8</sub>O<sub>12</sub>·3H<sub>2</sub>O: C, 54.64; H, 6.45; N, 9.44%. IR (KBr):  $\nu(\text{Ar-H})$  3058,  $\nu_{\text{as}}(\text{CH}_2)$  2935,  $\nu_{\text{s}}(\text{CH}_2)$  2792,  $\nu(\text{C=N})$  1620,  $\nu_{\text{as}}(\text{CO}_2^-)$  1558,  $\nu_{\text{s}}(\text{CO}_2^-)$  1446 cm<sup>-1</sup>. Diffuse reflectance spectrum:  $\lambda_{\text{max}}$  232, 284, 366, 707 nm. UV-vis:  $\lambda_{\text{max}}$  ( $\epsilon/\text{M}^{-1}\text{cm}^{-1}$ , measured in DMSO) 366 (14600), 664 (1020) nm.

**[Mn<sub>2</sub>(O<sub>2</sub>CCH<sub>3</sub>)<sub>2</sub>(tdtbsaec)]·5H<sub>2</sub>O (9·5H<sub>2</sub>O).** To a stirred solution of taec (30 mg, 0.08 mmol) in methanol (10 cm<sup>3</sup>) were added 3,5-di-*tert*-butylsalicylaldehyde (75 mg, 0.32 mmol) and a

Table 1. Crystal Data and Data Collection Details

	[Mn <sub>2</sub> (O <sub>2</sub> CCH <sub>3</sub> ) <sub>2</sub> (tbsaec)]· 2CHCl <sub>3</sub> ( <b>3</b> ·2CHCl <sub>3</sub> )	[Mn <sub>2</sub> (O <sub>2</sub> CC <sub>6</sub> H <sub>5</sub> ) <sub>2</sub> (tbsaec)] ( <b>4</b> )	[Mn <sub>2</sub> (O <sub>2</sub> CC <sub>6</sub> H <sub>5</sub> ) <sub>2</sub> (tcsaec)] ( <b>6</b> )	[Mn <sub>2</sub> (O <sub>2</sub> CCH <sub>3</sub> ) <sub>2</sub> (tmsaec)] ( <b>8</b> )
Formula	C <sub>52</sub> H <sub>60</sub> Br <sub>4</sub> Cl <sub>6</sub> Mn <sub>2</sub> N <sub>8</sub> O <sub>8</sub>	C <sub>60</sub> H <sub>62</sub> Br <sub>4</sub> Mn <sub>2</sub> N <sub>8</sub> O <sub>8</sub>	C <sub>60</sub> H <sub>62</sub> Cl <sub>4</sub> Mn <sub>2</sub> N <sub>8</sub> O <sub>8</sub>	C <sub>54</sub> H <sub>70</sub> Mn <sub>2</sub> N <sub>8</sub> O <sub>12</sub>
FW	1567.30	1452.70	1274.86	1133.06
Temperature/K	123	293	293	293
Crystal system	Monoclinic	Triclinic	Triclinic	Monoclinic
Space group	<i>P</i> 2 <sub>1</sub> / <i>c</i>	<i>P</i> $\bar{1}$	<i>P</i> $\bar{1}$	<i>P</i> 2 <sub>1</sub> / <i>n</i>
<i>a</i> /Å	14.002(3)	10.2688(16)	10.2036(19)	10.858(2)
<i>b</i> /Å	16.674(4)	10.9941(17)	11.003(2)	22.054(4)
<i>c</i> /Å	14.700(4)	14.136(2)	14.138(3)	12.590(3)
$\alpha$ /°		111.821(3)	112.408(4)	
$\beta$ /°	117.847(4)	93.270(3)	93.521(5)	108.342(4)
$\gamma$ /°		91.562(3)	91.220(4)	
<i>V</i> /Å <sup>3</sup>	3034.0(12)	1477.2(4)	1463.0(5)	2861.8(10)
<i>Z</i>	2	1	1	2
<i>D</i> <sub>calcd</sub> /g cm <sup>-3</sup>	1.72	1.63	1.45	1.32
<i>D</i> <sub>m</sub> /g cm <sup>-3</sup>	1.70	1.62	1.43	1.31
Crystal size/mm <sup>3</sup>	0.37 × 0.15 × 0.12	0.25 × 0.08 × 0.07	0.22 × 0.20 × 0.07	0.42 × 0.15 × 0.05
$\mu$ (Mo K $\alpha$ )/mm <sup>-1</sup>	3.372	3.194	0.677	0.507
$\theta$ range/°	1.64–28.63	1.56–28.47	1.56–28.40	1.85–28.43
No. of reflections	18656	9156	9014	17270
No. of unique reflections	7090	6542	6399	6565
<i>R</i> 1, <i>wR</i> 2 [ <i>I</i> > 2 $\sigma$ ( <i>I</i> )] <sup>a</sup>	0.0417, 0.0950	0.0581, 0.1158	0.0719, 0.1675	0.0759, 0.1391
Goodness-of-fit on <i>F</i> <sup>2</sup>	0.860	0.691	0.847	1.019

a)  $R1 = \Sigma ||F_o| - |F_c|| / \Sigma |F_o|$ ;  $wR2 = [\Sigma w(F_o^2 - F_c^2)^2 / \Sigma w(F_o^2)]^{1/2}$ .

methanol solution (5 cm<sup>3</sup>) of manganese(II) acetate tetrahydrate (39 mg, 0.16 mmol). The mixture was allowed to stand at room temperature to give dark green crystals. Yield: 71 mg (57%). Anal. Found: C, 63.25; H, 8.51; N, 6.91%. Calcd for C<sub>82</sub>H<sub>126</sub>Mn<sub>2</sub>N<sub>8</sub>O<sub>8</sub>·5H<sub>2</sub>O: C, 63.46; H, 8.83; N, 7.22%. IR (KBr):  $\nu_{as}(\text{CH}_2)$  2955,  $\nu_s(\text{CH}_2)$  2799,  $\nu(\text{C}=\text{N})$  1625,  $\nu_{as}(\text{CO}_2^-)$  1552,  $\nu_s(\text{CO}_2^-)$  1436 cm<sup>-1</sup>. Diffuse reflectance spectrum:  $\lambda_{\text{max}}$  229, 280sh, 376, 463sh, 757 nm. UV–vis:  $\lambda_{\text{max}}$  ( $\epsilon/\text{M}^{-1}\text{cm}^{-1}$ , measured in CHCl<sub>3</sub>) 270sh (43700), 372 (16700), 736 (1410) nm.

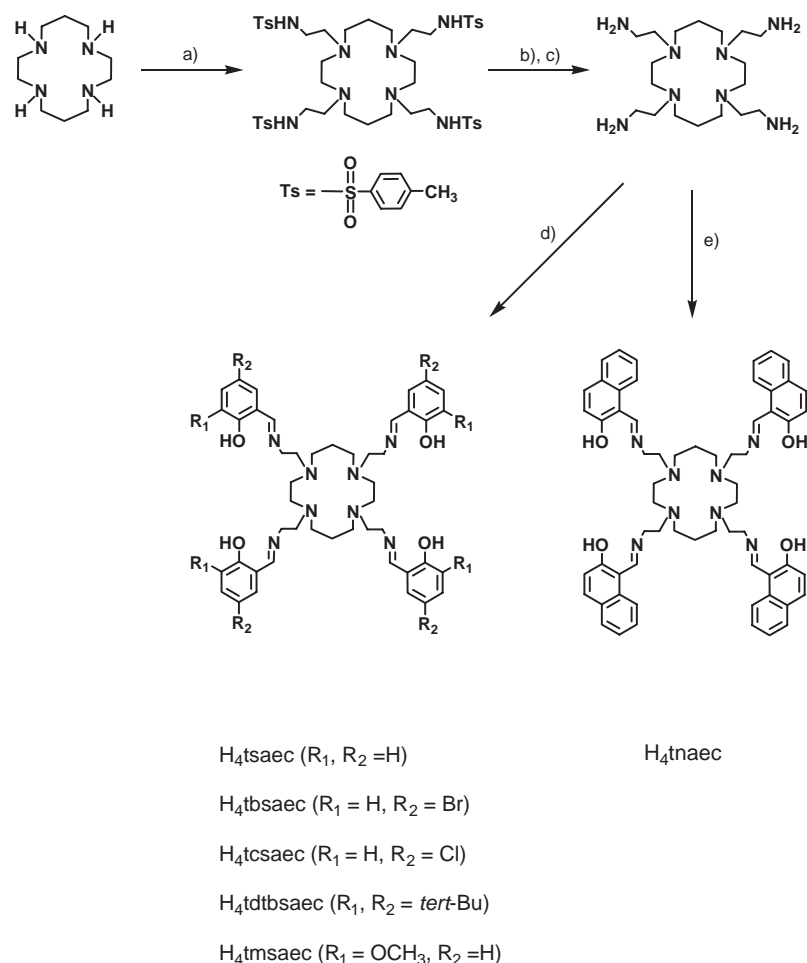
**[Mn<sub>2</sub>(O<sub>2</sub>CC<sub>6</sub>H<sub>5</sub>)<sub>2</sub>(tdtbsaec)]·3H<sub>2</sub>O (10·3H<sub>2</sub>O).** The complex was prepared in the same way as **9**, except that manganese(II) benzoate dihydrate was used instead of manganese(II) acetate tetrahydrate. Yield: 80 mg (61%). Anal. Found: C, 67.28; H, 8.24; N, 6.67%. Calcd for C<sub>92</sub>H<sub>130</sub>Mn<sub>2</sub>N<sub>8</sub>O<sub>8</sub>·3H<sub>2</sub>O: C, 67.38; H, 8.36; N, 6.83%. IR (KBr):  $\nu_{as}(\text{CH}_2)$  2953,  $\nu_s(\text{CH}_2)$  2793,  $\nu(\text{C}=\text{N})$  1621,  $\nu_{as}(\text{CO}_2^-)$  1535,  $\nu_s(\text{CO}_2^-)$  1437 cm<sup>-1</sup>. Diffuse reflectance spectrum:  $\lambda_{\text{max}}$  228, 271sh, 373, 462sh, 773 nm. UV–vis:  $\lambda_{\text{max}}$  ( $\epsilon/\text{M}^{-1}\text{cm}^{-1}$ , measured in CHCl<sub>3</sub>) 268 (46600), 373 (16400), 750 (1390) nm.

**Measurements.** Elemental analyses of carbon, hydrogen, nitrogen, and sulfur were conducted using a Thermo Finnigan FLASH EA 1112 series CHNO-S Analyzer. Infrared spectra were measured with a JASCO MFT-2000 FT-IR Spectrometer in the 4000–600 cm<sup>-1</sup> region. The electronic spectra were measured with a Shimadzu UV–vis–NIR Recording Spectrophotometer Model UV-3100. The temperature dependence of the magnetic susceptibilities was measured with a Quantum Design MPMS-5S SQUID susceptometer operating at a magnetic field of 0.5 T over a temperature range of 4.5–300 K. The susceptibilities were corrected for the diamagnetism of constituent atoms using Pascal's constants.<sup>13</sup> The effective magnetic moments were calculated from the equation  $\mu_{\text{eff}} = 2.828\sqrt{\chi_{\text{M}}T}$ , where  $\chi_{\text{M}}$  is the magnetic susceptibility per mole of Mn<sup>III</sup><sub>2</sub> dinuclear unit.

**X-ray Crystal Structure Analyses.** A preliminary examination was made, and data were collected on a Bruker CCD X-ray diffractometer (SMART APEX) using graphite-monochromated Mo K $\alpha$  radiation. Crystal data and details concerning data collection are given in Table 1. The structures were solved by direct methods and refined by full-matrix least-squares methods. The hydrogen atoms were inserted at their calculated positions and fixed there. All of the calculations were carried out on a Pentium IV Windows 2000 computer utilizing the SHELXTL software package.<sup>14</sup> Crystallographic data have been deposited with Cambridge Crystallographic Data Centre: Deposit numbers CCDC-641438–641442. Copies of the data can be obtained free of charge via <http://www.ccdc.cam.ac.uk/conts/retrieving.html> (or from the Cambridge Crystallographic Data Centre, 12, Union Road, Cambridge, CB2 1EZ, UK; Fax: +44 1223 336033; e-mail: deposit@ccdc.cam.ac.uk).

## Results and Discussion

**Schiff-Base Ligands.** The synthetic route for the present Schiff-base ligands is shown in Scheme 1. The analytical data are in good agreement with the theoretical requirements of the Schiff-base ligands. The ligands have a strong IR band at 1630–1635 cm<sup>-1</sup>, which is attributed to a  $\nu(\text{C}=\text{N})$  stretching vibration. Manganese complexes were prepared by the reaction of manganese(II) salts and the Schiff-base ligands in a 2:1 molar ratio in methanol, chloroform–methanol, or acetonitrile in good yields. In the cases of H<sub>4</sub>tsaec, H<sub>4</sub>tmsaec, and H<sub>4</sub>tdtbsaec, the reaction afforded an oily substance, and we could not obtain any solid products of the Schiff-base ligands by the same reaction as those of H<sub>4</sub>tbsaec, H<sub>4</sub>tcsaec, and H<sub>4</sub>tnaec. Therefore, we used a template reaction to prepare manganese complexes of these Schiff-base ligands. There is



Scheme 1. Reagents: a) *N*-Tosylaziridine/ $\text{CH}_3\text{CN}/81^\circ\text{C}/15\text{ h}$ . b)  $\text{HBr}/\text{CH}_3\text{COOH}/110^\circ\text{C}/40\text{ h}$ . c) Ion-exchange column. d) Salicylaldehyde derivatives/ $\text{CH}_3\text{OH}$ . e) 2-Hydroxy-1-naphthaldehyde/ $\text{CH}_3\text{OH}$ .

one vibration band in the IR spectra of the manganese complexes assignable to the coordinated  $\nu(\text{C}=\text{N})$  stretching vibration ( $1616\text{--}1625\text{ cm}^{-1}$ ), which is slightly shifted from the stretching band of the free Schiff-base ligand toward lower frequency by coordination to the metal ion. Elemental analyses confirmed the 1:2:2 deprotonated Schiff-base ligand:metal ion:anion stoichiometry of the manganese(III) complexes.

**Dinuclear Manganese(III) Complexes with Acetate or Benzoate as the Additional Ligands,  $[\text{Mn}_2(\text{O}_2\text{CCH}_3)_2(\text{L})]$  [ $\text{L} = \text{tsaec}$  (1),  $\text{tbsaec}$  (3),  $\text{tcsaec}$  (5),  $\text{tmsaec}$  (8),  $\text{tdtbsaec}$  (9)] and  $[\text{Mn}_2(\text{O}_2\text{CC}_6\text{H}_5)_2(\text{L})]$  [ $\text{L} = \text{tsaec}$  (2),  $\text{tbsaec}$  (4),  $\text{tcsaec}$  (6),  $\text{tdtbsaec}$  (10)].** When manganese(II) acetate or manganese(II) benzoate was reacted with the Schiff-base ligands, dinuclear manganese(III) complexes,  $[\text{Mn}_2(\text{O}_2\text{CCH}_3)_2(\text{L})]$  ( $\text{L} = \text{tsaec}$  (1),  $\text{tbsaec}$  (3),  $\text{tcsaec}$  (5),  $\text{tmsaec}$  (8),  $\text{tdtbsaec}$  (9)) and  $[\text{Mn}_2(\text{O}_2\text{CC}_6\text{H}_5)_2(\text{L})]$  ( $\text{L} = \text{tsaec}$  (2),  $\text{tbsaec}$  (4),  $\text{tcsaec}$  (6),  $\text{tdtbsaec}$  (10)) were isolated in good yields (46–71%). In the IR spectra of these complexes, two strong vibration peaks of carboxylato groups appear at  $1535\text{--}1561$  and  $1436\text{--}1461\text{ cm}^{-1}$ , which are attributed to the antisymmetric and symmetric  $\nu(\text{CO}_2^-)$  stretching bands, respectively. The  $\Delta$  values of  $\nu_{\text{as}}(\text{CO}_2^-) - \nu_{\text{s}}(\text{CO}_2^-)$  are in the range of those of bidentate-acetate complexes.<sup>15</sup>

Single crystals suitable for X-ray diffraction study were ob-

tained for  $[\text{Mn}_2(\text{O}_2\text{CCH}_3)_2(\text{tbsaec})] \cdot 2\text{CHCl}_3$  (**3**· $2\text{CHCl}_3$ ),  $[\text{Mn}_2(\text{O}_2\text{CCH}_3)_2(\text{tmsaec})]$  (**8**),  $[\text{Mn}_2(\text{O}_2\text{CC}_6\text{H}_5)_2(\text{tbsaec})]$  (**4**), and  $[\text{Mn}_2(\text{O}_2\text{CC}_6\text{H}_5)_2(\text{tcsaec})]$  (**6**). The crystal structures of these complexes were determined by X-ray crystal structure analysis. An ORTEP drawing of the molecular structure of **3**· $2\text{CHCl}_3$  is shown in Fig. 1. Selected bond distances and angles are listed in Table 2. The structure is very similar to that of a previously reported dinuclear manganese(III) complex,  $[\text{Mn}_2(\text{O}_2\text{CCH}_3)_2(\text{tcsaec})] \cdot 2\text{CHCl}_3$  (**5**· $2\text{CHCl}_3$ ).<sup>12</sup> The asymmetric unit contains one-half of the dinuclear unit with the cyclam-ring moiety centered on a crystallographic inversion center. Two pairs of the pendant groups point away from the cyclam ring, forming an extended conformation. It should be noted that the cyclam ring moiety takes the *trans* IV form,<sup>4</sup> which has never been found in metal complexes of taec (the word “*trans* III” in Ref. 12a should be corrected to “*trans* IV”).<sup>3</sup> The two manganese ions are bound to the two pendant Schiff-base groups in a *cis-α* fashion<sup>16</sup> (the word “*cis-β*” in Ref. 12a should be corrected to “*cis-α*”) below and above the cyclam ring moiety. The distance between the two manganese ions ( $\text{Mn1} \cdots \text{Mn1}'$ ) is  $10.096(2)\text{ \AA}$ . Each manganese ion is coordinated by two imino-nitrogen atoms and two phenoxo-oxygen atoms of two 5-bromosalicylideneaminoethyl pendant arms of  $\text{tbsaec}^{4-}$  and two oxygen atoms of the bidentate ace-

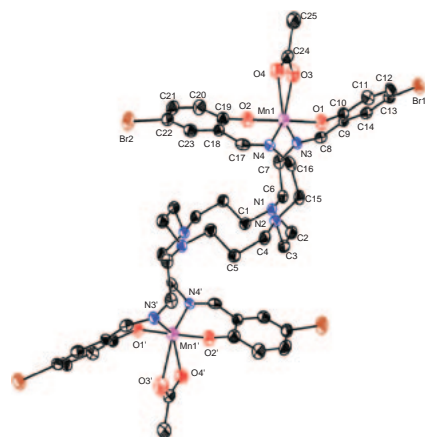


Fig. 1. ORTEP drawing of the structure of  $[\text{Mn}_2(\text{O}_2\text{CCH}_3)_2(\text{tbsaec})] \cdot 2\text{CHCl}_3$  (**3**· $2\text{CHCl}_3$ ) showing the 50% probability thermal ellipsoids and atom labeling scheme. Hydrogen atoms are omitted for clarity.

tate ligand. The manganese ion (Mn1) lies 0.031 Å above the plane described by the two imino-nitrogen atoms (N3, N4) and the acetato-oxygen atoms (O3, O4). The coordination geometry can be regarded as an axial compressed octahedron with two short bonds with phenoxo-oxygen atoms (Mn1–O1 = 1.863(2) Å, Mn1–O2 = 1.855(3) Å) and four long bonds with imino-nitrogen and acetato-oxygen atoms (Mn1–O3 = 2.195(3) Å, Mn1–O4 = 2.253(3) Å, Mn1–N3 = 2.105(3) Å, Mn1–N4 = 2.102(3) Å), in contrast to the fact that most manganese(III) complexes show axially elongated octahedra for  $\text{Mn}^{\text{III}}$  centers.<sup>5,6</sup> This may be ascribed to the combination of the pseudo Jahn–Teller distortion of a high-spin  $d^4$  ion and the preference of  $\text{Mn}^{\text{III}}$  for phenoxo-oxygen donors over imino-nitrogen and acetato-oxygen donor atoms.<sup>17</sup> The tetradentate  $\text{N}_2\text{O}_2$  Schiff-base moiety is not planar in this complex; the dihedral angle between the two salicylideneamino planes defined by O1–C10–C11–C12–C13–C14–C9–C8 and O2–C19–C20–C21–C22–C23–C18–C17 is 48.0°. Therefore, the plane defined by O1–N3–N4–O2 deviates from the planar configuration within  $\pm 0.48$  Å, and the manganese ion is 0.49 Å above this mean plane. A view of the molecular packing in the crystal is shown in Fig. 2. The closest intermolecular Mn...Mn distance is 6.795(2) Å of Mn1...Mn1 ( $-x+1, -y+1, -z+1$ ), which is shorter than the intramolecular Mn...Mn distance. The crystal contains chloroform molecules, which form hydrogen bonds with the acetate ligands [O4 ( $\text{O}_2\text{CCH}_3$ )...C26 ( $\text{CHCl}_3$ ) ( $-x+1, y+0.5, -z+0.5$ ) 3.036(5) Å].

ORTEP drawings of the crystal structures of **8**, **4**, and **6** are shown in Figs. 3, 4, and 5, respectively. The structures of **8**, **4**, and **6** are similar to those of **3**· $2\text{CHCl}_3$  and **5**· $2\text{CHCl}_3$ , namely, the coordination geometry is a similar compressed octahedron with two shorter Mn–phenoxo bonds and four longer bonds with imino-nitrogen and carboxylato-oxygen atoms (Table 2). The intramolecular Mn1...Mn1' distances are 9.988(2), 9.865(3), and 9.847(3) Å, for **8**, **4**, and **6**, respectively. Although the coordination modes of the carboxylato ligands are unsymmetrically bidentate, being different from those of **3**· $2\text{CHCl}_3$  and **5**· $2\text{CHCl}_3$ , the IR spectra of these complexes exhibit absorptions indicative of the bidentate nature of the carboxylato groups.<sup>15</sup> For **4** and **6**, the manga-

Table 2. Selected Bond Distances (Å) and Angles (°) with Their Estimated Standard Deviations in Parentheses

$[\text{Mn}_2(\text{O}_2\text{CCH}_3)_2(\text{tbsaec})] \cdot 2\text{CHCl}_3$ ( <b>3</b> · $2\text{CHCl}_3$ )			
Mn1–O1	1.863(2)	Mn1–O4	2.253(3)
Mn1–O2	1.855(3)	Mn1–N3	2.105(3)
Mn1–O3	2.195(3)	Mn1–N4	2.102(3)
O1–Mn1–O2	178.4(1)	O2–Mn1–N3	91.0(1)
O1–Mn1–O3	89.8(1)	O2–Mn1–N4	90.3(1)
O1–Mn1–O4	90.3(1)	O3–Mn1–N3	87.8(1)
O2–Mn1–O3	91.1(1)	O3–Mn1–N4	146.4(1)
O2–Mn1–O4	91.3(1)	O4–Mn1–N3	146.5(1)
O3–Mn1–O4	58.8(1)	O4–Mn1–N4	87.7(1)
O1–Mn1–N3	87.7(1)	N3–Mn1–N4	125.7(1)
O1–Mn1–N4	89.7(1)		
$[\text{Mn}_2(\text{O}_2\text{CC}_6\text{H}_5)_2(\text{tbsaec})]$ ( <b>4</b> )			
Mn1–O1	1.843(5)	Mn1–O4	2.513(6)
Mn1–O2	1.891(5)	Mn1–N3	2.087(5)
Mn1–O3	2.130(5)	Mn1–N4	2.135(6)
O1–Mn1–O2	176.4(2)	O2–Mn1–N3	89.7(2)
O1–Mn1–O3	88.6(2)	O2–Mn1–N4	85.8(2)
O1–Mn1–O4	80.0(2)	O3–Mn1–N3	138.8(2)
O2–Mn1–O3	94.5(2)	O3–Mn1–N4	90.7(2)
O2–Mn1–O4	103.3(2)	O4–Mn1–N3	83.8(2)
O3–Mn1–O4	55.3(2)	O4–Mn1–N4	145.0(2)
O1–Mn1–N3	89.1(2)	N3–Mn1–N4	130.5(2)
O1–Mn1–N4	92.3(2)		
$[\text{Mn}_2(\text{O}_2\text{CC}_6\text{H}_5)_2(\text{tcsaec})]$ ( <b>6</b> )			
Mn1–O1	1.830(4)	Mn1–O4	2.482(6)
Mn1–O2	1.884(4)	Mn1–N3	2.085(5)
Mn1–O3	2.128(5)	Mn1–N4	2.123(5)
O1–Mn1–O2	176.7(2)	O2–Mn1–N3	89.9(2)
O1–Mn1–O3	88.1(2)	O2–Mn1–N4	86.2(2)
O1–Mn1–O4	80.5(2)	O3–Mn1–N3	139.4(2)
O2–Mn1–O3	94.5(2)	O3–Mn1–N4	90.2(2)
O2–Mn1–O4	102.6(2)	O4–Mn1–N3	83.8(2)
O3–Mn1–O4	55.8(2)	O4–Mn1–N4	145.1(2)
O1–Mn1–N3	89.4(2)	N3–Mn1–N4	130.4(2)
O1–Mn1–N4	91.9(2)		
$[\text{Mn}_2(\text{O}_2\text{CCH}_3)_2(\text{tmsaec})]$ ( <b>8</b> )			
Mn1–O1	1.867(3)	Mn1–O6	2.466(3)
Mn1–O3	1.852(3)	Mn1–N3	2.151(3)
Mn1–O5	2.063(3)	Mn1–N4	2.059(3)
O1–Mn1–O3	177.3(1)	O3–Mn1–N3	91.2(1)
O1–Mn1–O5	91.8(1)	O3–Mn1–N4	89.6(1)
O1–Mn1–O6	95.2(1)	O5–Mn1–N3	91.9(1)
O3–Mn1–O5	89.9(1)	O5–Mn1–N4	144.4(1)
O3–Mn1–O6	87.5(1)	O6–Mn1–N3	148.7(1)
O5–Mn1–O6	56.9(1)	O6–Mn1–N4	87.5(1)
O1–Mn1–N3	86.7(1)	N3–Mn1–N4	123.7(1)
O1–Mn1–N4	90.2(1)		

nese(III) ion lies 0.05 Å above the mean plane described by the two imino-nitrogen atoms (N3 and N4) and the two benzoato-oxygen atoms (O3 and O4). The dihedral angles between the two salicylideneamino planes defined by O1–C10–

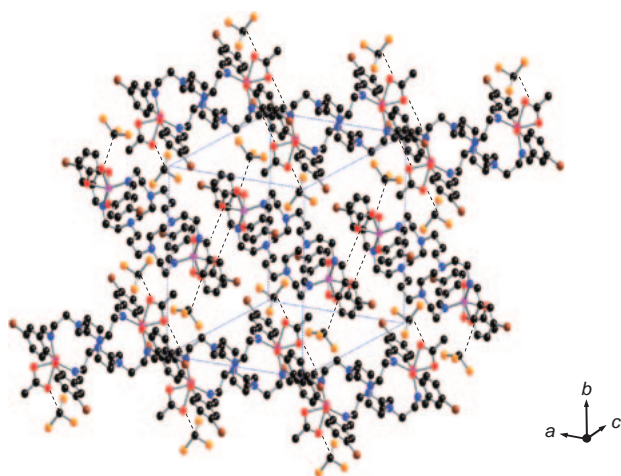


Fig. 2. Packing diagram of  $[\text{Mn}_2(\text{O}_2\text{CCH}_3)_2(\text{tbsaec})] \cdot 2\text{CHCl}_3$  (**3**· $2\text{CHCl}_3$ ). Hydrogen atoms are omitted for clarity.

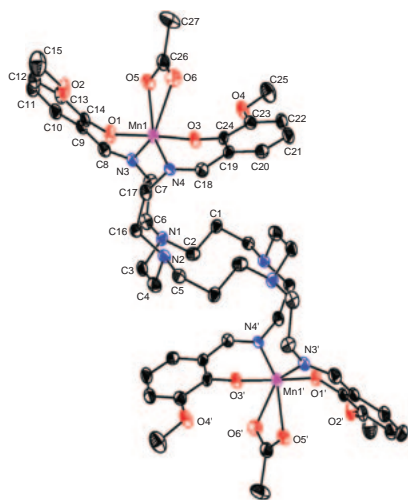


Fig. 3. ORTEP drawing of the structure of  $[\text{Mn}_2(\text{O}_2\text{CCH}_3)_2(\text{tmsaec})]$  (**8**) showing the 40% probability thermal ellipsoids and atom labeling scheme. Hydrogen atoms are omitted for clarity.

$\text{C11-C12-C13-C14-C9-C8}$  and  $\text{O2-C19-C20-C21-C22-C23-C18-C17}$  are  $42.0$  and  $42.9^\circ$  for **4** and **6**, respectively. The planes defined by the two imino-nitrogen atoms ( $\text{N3}$  and  $\text{N4}$ ) and the two phenoxo-oxygen atoms ( $\text{O1}$  and  $\text{O2}$ ) are distorted from the plane by  $\pm 0.42 \text{ \AA}$ , and the manganese ion is  $0.47 \text{ \AA}$  above the mean planes for both the complexes. In the case of **8**, the tetradentate  $\text{N}_2\text{O}_2$  Schiff-base moiety is severely distorted, with a dihedral angle between the two salicylidene-amino planes defined by  $\text{O1-C14-C13-C12-C11-C10-C9-C8}$  and  $\text{O3-C24-C23-C22-C21-C20-C19-C18}$  of  $60.0^\circ$ , which is the largest of the present complexes. This may be due to the steric hindrance of the 3-methoxy groups of  $\text{tmsaec}^{4-}$ . Similarly, the plane defined by  $\text{O1-N3-N4-O3}$  is distorted from the plane by  $\pm 0.49 \text{ \AA}$  and the manganese ion being  $0.52 \text{ \AA}$  above the mean plane. In the crystals, the closest intermolecular  $\text{Mn} \cdots \text{Mn}$  separations are  $7.873(3) \text{ \AA}$  of  $\text{Mn1} \cdots \text{Mn1} (-x, -y + 1, -z + 1)$  for **4**,  $6.882(3) \text{ \AA}$  of  $\text{Mn1} \cdots \text{Mn1} (-x + 1, -y + 1, -z + 1)$  for **6**, and  $6.899(2) \text{ \AA}$  of  $\text{Mn1} \cdots \text{Mn1} (-x,$

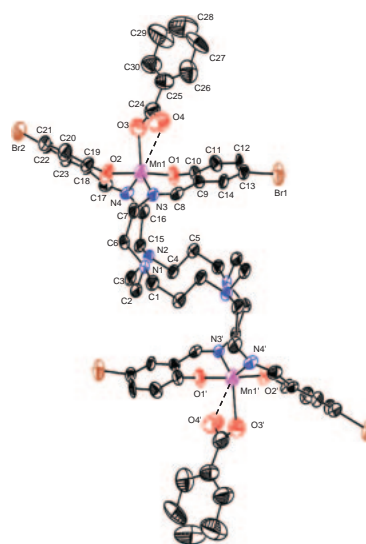


Fig. 4. ORTEP drawing of the structure of  $[\text{Mn}_2(\text{O}_2\text{CC}_6\text{H}_5)_2(\text{tbsaec})]$  (**4**) showing the 45% probability thermal ellipsoids and atom labeling scheme. Hydrogen atoms are omitted for clarity.

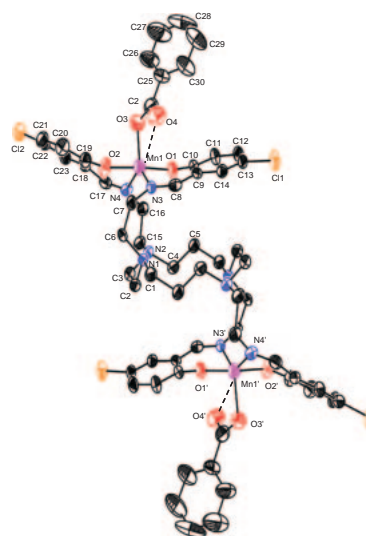


Fig. 5. ORTEP drawing of the structure of  $[\text{Mn}_2(\text{O}_2\text{CC}_6\text{H}_5)_2(\text{tcsaec})]$  (**6**) showing the 40% probability thermal ellipsoids and atom labeling scheme. Hydrogen atoms are omitted for clarity.

$-y + 2, -z)$  for **8**, respectively.

**Dinuclear Manganese(III) Complex with Azide as the Additional Ligands,  $[\text{Mn}_2(\text{N}_3)_2(\text{tnaec})]$  (**7**).** When manganese(II) acetate was reacted with the  $\text{tnaec}$  ligand in chloroform-methanol, the reaction solution became yellowish brown. However, the solution did not afford any precipitate even after standing for months at room temperature. This contrasts with the case for the corresponding salen type Schiff-base, bis(2-hydroxy-1-naphthylmethylidene)ethylenediamine ( $\text{Hbne}$ ), which forms a polymeric catena- $\mu$ -acetatomanganese(III) complex with  $\text{bne}$ ,  $[\text{Mn}(\text{O}_2\text{CCH}_3)(\text{bne})]_n$ .<sup>18</sup> By adding azide ion to the solution, we isolated a dinuclear manganese(III) complex,  $[\text{Mn}_2(\text{N}_3)_2(\text{tnaec})]$  (**7**), in good yield (61%). The IR spectrum of **7** showed a strong band at  $2038 \text{ cm}^{-1}$ ,



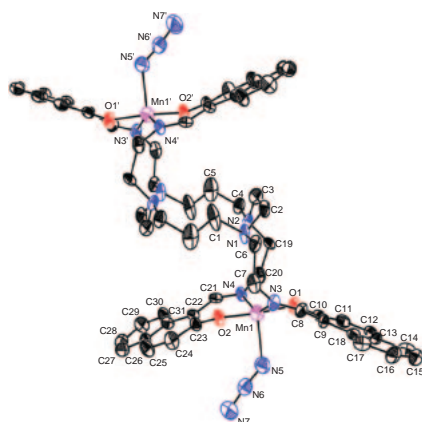


Fig. 6. ORTEP drawing of the structure of  $[\text{Mn}_2(\text{N}_3)_2(\text{tnac})] \cdot 2\text{CHCl}_3$  (**7**· $2\text{CHCl}_3$ ) showing the 25% probability thermal ellipsoids and atom labeling scheme. Hydrogen atoms are omitted for clarity.

which was assigned to the asymmetric stretching vibration of the terminal azide group,<sup>15</sup> in good accord with the structural results (vide infra). In the case of manganese complexes, most azide complexes have  $\text{N}_3^-$  bridges. Only a few structurally characterized complexes of  $\text{Mn}^{\text{III}}$  having terminal  $\text{N}_3^-$  ligands have been reported.<sup>8h,19</sup> Unfortunately, we failed to obtain satisfactory crystallographic data and therefore a more detailed analysis of the structure of **7** could not be attained.<sup>20</sup> An ORTEP drawing of the preliminary X-ray crystal structure of **7**· $2\text{CHCl}_3$  is shown in Fig. 6. The manganese(III) ion is coordinated by two imino-nitrogen atoms, two phenoxo-oxygen atoms from  $\text{tnac}^{4-}$ , and one nitrogen atom from azide ligand, forming a trigonal bipyramidal geometry. The axial sites are occupied by the phenoxo-oxygen atoms (O1 and O2), with shorter bond lengths ( $\text{Mn1-O1} = 1.835(7)$ ,  $\text{Mn1-O2} = 1.856(7)$  Å) compared with the equatorial Mn–N distances ( $\text{Mn1-N3} = 2.055(8)$ ,  $\text{Mn1-N4} = 2.002(9)$ ,  $\text{Mn1-N5} = 2.064(12)$  Å). These bond distances should be considered with some care because of the low accuracy of this structure analysis. The intramolecular Mn1...Mn1' distance is 9.676(4) Å. In the crystal, the closest intermolecular Mn...Mn separation is 8.063(5) Å between Mn1...Mn1' ( $-x + 1/2, -y + 3/2, -z + 1$ ).

**Electronic Spectra of Complexes 1–10.** The UV–visible spectra of the present complexes were measured by diffuse reflectance spectra, because most of them are insoluble in water and organic solvents. The diffuse reflectance spectra of **1**, **2**, and **7** are shown in Fig. 7 as examples. The spectra of the acetates and the benzoates are almost identical, confirming the similar coordination environments. The complexes exhibited two or three strong bands (226–236, 255–284, and 360–376 nm) in the UV region and a band at 705–773 nm with shoulder at 438–540 nm in the visible region. In  $\text{CHCl}_3$  solution, acetate complex **9** showed three absorptions at 270sh, 372, and 736 nm with molar extinction coefficients of 21850, 8350, and 705  $\text{dm}^3 \text{mol}^{-1} \text{cm}^{-1}/\text{Mn}$ , respectively. Judging from the intensities of the absorption bands, we assigned the lowest-energy broad band at 705–773 nm to d–d transition bands for  $\text{Mn}^{\text{III}}$  ion in a compressed octahedral environment.<sup>17</sup> The shoulder band around 438–540 was assigned by analogy to other manganese(III) complexes to be a LMCT band from the phenoxo-

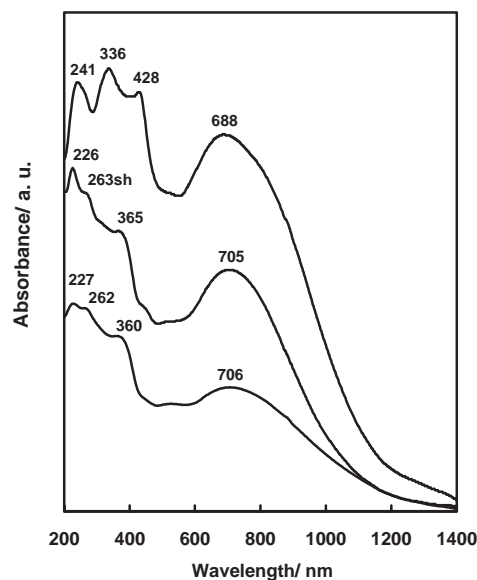


Fig. 7. Diffuse reflectance spectra of  $[\text{Mn}_2(\text{O}_2\text{CCH}_3)_2(\text{tsaec})]$  (**1**) (bottom),  $[\text{Mn}_2(\text{O}_2\text{CC}_6\text{H}_5)_2(\text{tsaec})]$  (**2**) (middle), and  $[\text{Mn}_2(\text{N}_3)_2(\text{tnac})]$  (**7**) (top).

oxygen to the  $\text{Mn}^{\text{III}}$  d orbitals.<sup>17,21</sup>

In the case of azide complex **7**, the diffuse reflectance spectra had four bands at 241, 336, 428, and 688 nm. Compared to those of the acetates and benzoates, the distinctive bands at 336 and 428 nm were assigned to the  $\pi$ – $\pi^*$  transition of coordinated azide ligands and the  $\text{N}_3$ –Mn charge-transfer bands, tentatively.<sup>19b,19c</sup> In DMSO solution, the azide complex exhibited five absorptions at 308, 330sh, 402, 422, and 625 nm with molar extinction coefficients of 17500, 15800, 8050, 7350, and 434  $\text{dm}^3 \text{mol}^{-1} \text{cm}^{-1}/\text{Mn}$ , respectively. Similar to the acetates and benzoates, the lowest band at 688 nm was assigned to d–d transition bands for the five-coordinate  $\text{Mn}^{\text{III}}$  ion.

**Magnetic Properties of Complexes 1–10.** The temperature dependence of the magnetic susceptibilities of **1–10** was measured on powdered samples in the temperature range of 4.5–300 K. The magnetic data of **3**, **8**, and **7** are shown in Figs. 8, 9, and 10, respectively, in the form of  $\chi_{\text{M}}$  and  $\mu_{\text{eff}}$  vs.  $T$  plots as representative examples. The magnetic moments of these complexes at 300 K were in the range of 6.27–6.97  $\mu_{\text{B}}$  (per  $\text{Mn}^{\text{III}}_2$  unit) and are in good agreement with the spin-only value (6.93  $\mu_{\text{B}}$ ) of two noninteracting high-spin  $\text{Mn}^{\text{III}}$  ( $S = 2$ ) ions. For complexes **1–6**, **8**, and **9**, the magnetic moments remained constant upon lowering of the temperature to the range of 5–20 K, suggesting almost no magnetic interaction between manganese(III) ions. When the temperature was lowered further, the magnetic moment decreased for these complexes, which is thought to be due to the zero-field-splitting from the manganese(III) ion or antiferromagnetic intermolecular interactions. In the case of **7** and **10**, the magnetic moment slightly increased as the temperature decreased from 300 to 4.5 K, suggesting a weak ferromagnetic interaction between manganese(III) ions. In order to evaluate the magnetic behaviors described above, the magnetic data were analyzed with the van Vleck equation based on the Heisenberg model ( $H = -2JS_1 \cdot S_2$  ( $S_1 = S_2 = 2$ )):<sup>22</sup>

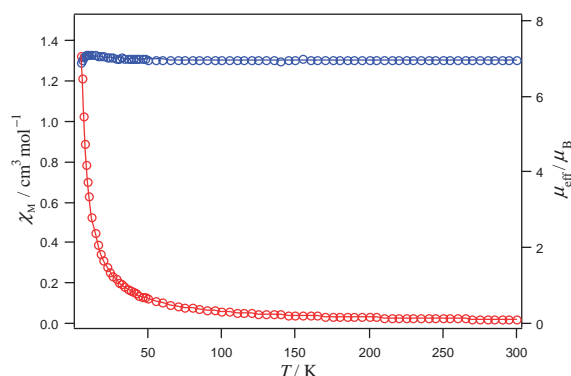


Fig. 8. Temperature dependence of magnetic susceptibility and effective magnetic moment of  $[\text{Mn}_2(\text{O}_2\text{CCH}_3)_2\text{-(tbsaac)}]$  (**3**). Solid line was drawn with the parameters  $g = 2.00$ ,  $J = +0.53 \text{ cm}^{-1}$ ,  $\theta = -2.3 \text{ K}$  for Eq. 1.

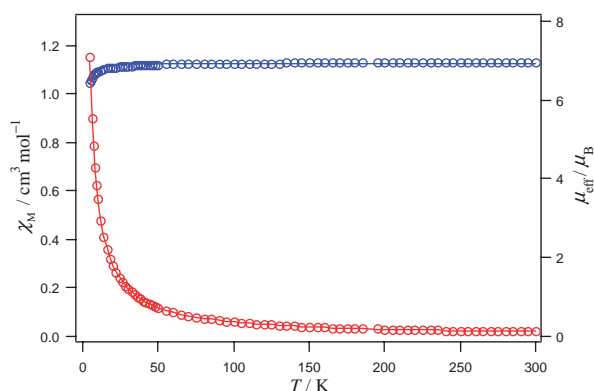


Fig. 9. Temperature dependence of magnetic susceptibility and effective magnetic moment of  $[\text{Mn}_2(\text{O}_2\text{CCH}_3)_2\text{-(tmsaac)}]$  (**8**). Solid line was drawn with the parameters  $g = 2.00$ ,  $D = +3.9 \text{ cm}^{-1}$  for Eq. 2.

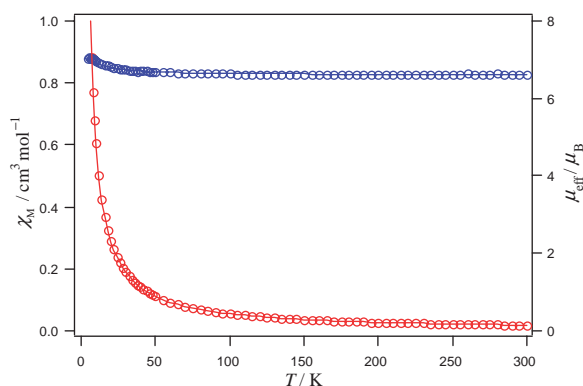


Fig. 10. Temperature dependence of magnetic susceptibility and effective magnetic moment of  $[\text{Mn}_2(\text{N}_3)_2\text{-(tnaec)}]$  (**7**). Solid line was drawn with the parameters  $g = 1.91$ ,  $D = -3.3 \text{ cm}^{-1}$ ,  $zJ = +0.17 \text{ cm}^{-1}$  for Eqs. 2–5.

$$\begin{aligned} \chi_M = & 2Ng^2\mu_B^2/k(T - \theta)[30 + 14\exp(-8J/kT) \\ & + 5\exp(-14J/kT) \\ & + \exp(-18J/kT)]/[9 + 7\exp(-8J/kT) \\ & + 5\exp(-14J/kT) + 3\exp(-18J/kT) \\ & + \exp(-20J/kT)], \end{aligned} \quad (1)$$

where  $J$  is an exchange integral for the two manganese(III) ions and the other symbols have their usual meanings. The best-fitting parameters obtained were as follows (Fig. 8):  $g = 2.02$ ,  $J = -0.16 \text{ cm}^{-1}$ ,  $\theta = +0.69 \text{ K}$  for **1**;  $g = 1.93$ ,  $J = -0.09 \text{ cm}^{-1}$ ,  $\theta = +0.50 \text{ K}$  for **2**;  $g = 2.00$ ,  $J = +0.53 \text{ cm}^{-1}$ ,  $\theta = -2.3 \text{ K}$  for **3**;  $g = 1.87$ ,  $J = +0.54 \text{ cm}^{-1}$ ,  $\theta = -2.8 \text{ K}$  for **4**;  $g = 1.96$ ,  $J = -0.23 \text{ cm}^{-1}$ ,  $\theta = +0.78 \text{ K}$  for **5**;  $g = 1.88$ ,  $J = -0.20 \text{ cm}^{-1}$ ,  $\theta = +0.73 \text{ K}$  for **6**;  $g = 1.90$ ,  $J = +0.49 \text{ cm}^{-1}$ ,  $\theta = -1.3 \text{ K}$  for **7**;  $g = 2.01$ ,  $J = +0.26 \text{ cm}^{-1}$ ,  $\theta = -2.3 \text{ K}$  for **8**;  $g = 1.91$ ,  $J = -0.14 \text{ cm}^{-1}$ ,  $\theta = +0.69 \text{ K}$  for **9**;  $g = 1.86$ ,  $J = +0.55 \text{ cm}^{-1}$ ,  $\theta = -1.5 \text{ K}$  for **10**. The obtained  $J$  values are very small, showing that the magnetic interaction within the dinuclear molecule can be negligibly weak. In our system, we did not expect any significant magnetic interaction between the two manganese(III) ions because of the long Mn...Mn distance and the intervening saturated macrocyclic ring. Compared with the  $J$  values, the absolute values of  $\theta$  values are definitely larger. These facts suggest that a zero-field-splitting of isolated manganese(III) ion cannot be excluded in the present cases. Thus, we analyzed the magnetic data by using the following equations based on two isolated  $S = 2$  ions with a zero-field-splitting as the first approximation:<sup>23,24</sup>

$$\chi_M = 2(2\chi_x + \chi_z)/3, \quad (2)$$

with

$$\begin{aligned} \chi_x = & (Ng^2\mu_B^2/kT)[(6kT/D)(1 - \exp(-D/kT)) \\ & + (4kT/3D)(\exp(-D/kT) \\ & - \exp(-4D/kT))]/[1 + 2\exp(-D/kT) \\ & + 2\exp(-4D/kT)], \end{aligned} \quad (3)$$

and

$$\begin{aligned} \chi_z = & (Ng^2\mu_B^2/kT)[2\exp(-D/kT) \\ & + 8\exp(-4D/kT)]/[1 + 2\exp(-D/kT) \\ & + 2\exp(-4D/kT)], \end{aligned} \quad (4)$$

where  $D$  is the zero-field-splitting parameter. As shown in Fig. 9, this model reproduced the magnetic data satisfactorily with the following parameters:  $g = 2.02$ ,  $D = -2.1 \text{ cm}^{-1}$  (or  $+2.3 \text{ cm}^{-1}$ ) for **1**;  $g = 1.93$ ,  $D = -1.0 \text{ cm}^{-1}$  (or  $+1.1 \text{ cm}^{-1}$ ) for **2**;  $g = 2.01$ ,  $D = -0.02 \text{ cm}^{-1}$  (or  $+0.02 \text{ cm}^{-1}$ ) for **3**;  $g = 1.87$ ,  $D = -1.9 \text{ cm}^{-1}$  (or  $+2.0 \text{ cm}^{-1}$ ) for **4**;  $g = 1.96$ ,  $D = -3.3 \text{ cm}^{-1}$  (or  $+3.7 \text{ cm}^{-1}$ ) for **5**;  $g = 1.88$ ,  $D = -2.7 \text{ cm}^{-1}$  (or  $+3.0 \text{ cm}^{-1}$ ) for **6**;  $g = 2.00$ ,  $D = -3.5 \text{ cm}^{-1}$  (or  $+3.9 \text{ cm}^{-1}$ ) for **8**;  $g = 1.91$ ,  $D = -1.4 \text{ cm}^{-1}$  (or  $+1.5 \text{ cm}^{-1}$ ) for **9**. The  $D$  values are in the range of those found in high-spin manganese(III) complexes ( $|D| \leq 8 \text{ cm}^{-1}$ ),<sup>25,26</sup> although the sign of  $D$  cannot be determined from the powder magnetic susceptibility data. For **7** and **10**, this model does not explain the increase in the magnetic moments in the low-temperature region, which is thought to be due to intermolecular interactions. In order to describe the intermolecular interactions, a molecular field approximation was introduced:<sup>24</sup>

$$\chi_M' = \chi_M/(1 - 2zJ\chi_M/Ng^2\mu_B^2). \quad (5)$$

Using Eqs. 2–5 the magnetic data of **7** and **10** were analyzed, and the best-fit parameters were as follows (Fig. 10):  $g = 1.91$ ,  $D = -3.3 \text{ cm}^{-1}$ ,  $zJ = +0.17 \text{ cm}^{-1}$  (or  $g = 1.90$ ,  $D =$



+6.1 cm<sup>-1</sup>,  $\nu J = +0.27$  cm<sup>-1</sup>) for **7**;  $g = 1.87$ ,  $D = -3.3$  cm<sup>-1</sup>,  $\nu J = +0.17$  cm<sup>-1</sup> (or  $g = 1.86$ ,  $D = +6.8$  cm<sup>-1</sup>,  $\nu J = +0.29$  cm<sup>-1</sup>) for **10**. The positive  $\nu J$  values suggest a weak ferromagnetic intermolecular interaction in these complexes.

### Conclusion

The new Schiff-base ligands, 1,4,8,11-tetrakis(salicylidene-aminoethyl)-1,4,8,11-tetraazacyclotetradecane (H<sub>4</sub>tsaec) and its substituent derivatives, were shown to be good ligands for the synthesis of a series of manganese(III) complexes with well-separated dinuclear systems having a long Mn...Mn distance of 9.676(4)–10.096(2) Å, which show essentially no magnetic interaction. This type of manganese complexes is unique and involves an undeveloped region of the dinuclear metal systems that have a nano-level metal...metal separation, although they do not seem to be model compounds for the OEC of PS-II.

The present work was partially supported by the "Open Research Center" Project for Private Universities: matching fund subsidy and Grants-in-Aid for Scientific Research Nos. 16550062 and 19550074 from the Ministry of Education, Culture, Sports, Science and Technology.

### References

- a) D. Parker, *Chem. Soc. Rev.* **1990**, 19, 271. b) P. V. Bernhardt, G. A. Lawrance, *Coord. Chem. Rev.* **1990**, 104, 297. c) S. Jurisson, D. Berning, W. Jia, D. Ma, *Chem. Rev.* **1993**, 93, 1137. d) V. Alexander, *Chem. Rev.* **1995**, 95, 273. e) K. P. Wainwright, *Coord. Chem. Rev.* **1997**, 166, 35. f) M. Meyer, V. Dahanoui-Gindrey, C. Lecomte, R. Guilard, *Coord. Chem. Rev.* **1998**, 178–180, 1313. g) I. Lukes, J. Kotek, P. Vojtisek, P. Hermann, *Coord. Chem. Rev.* **2001**, 216–217, 287. h) E. Toth, L. Helm, A. E. Merbach, in *Comprehensive Coordination Chemistry II*, ed. by J. A. McCleverty, T. J. Meyer, Elsevier, Amsterdam, **2004**, Vol. 9, pp. 841–881.
- R. Delgado, S. Quintino, M. Teixeira, A. Zhang, *J. Chem. Soc., Dalton Trans.* **1997**, 55.
- a) I. Murase, M. Mikuriya, H. Sonoda, S. Kida, *J. Chem. Soc., Chem. Commun.* **1984**, 692. b) I. Murase, M. Mikuriya, H. Sonoda, Y. Fukuda, S. Kida, *J. Chem. Soc., Dalton Trans.* **1986**, 953. c) S. Kida, I. Murase, C. Harada, L. Daizeng, M. Mikuriya, *Bull. Chem. Soc. Jpn.* **1986**, 59, 2595. d) M. Mikuriya, S. Kida, I. Murase, *J. Chem. Soc., Dalton Trans.* **1987**, 1261. e) M. Mikuriya, S. Kida, I. Murase, *Bull. Chem. Soc. Jpn.* **1987**, 60, 1355. f) M. Mikuriya, S. Kida, I. Murase, *Bull. Chem. Soc. Jpn.* **1987**, 60, 1681. g) M. Mikuriya, S. Kida, T. Kohzuma, I. Murase, *Bull. Chem. Soc. Jpn.* **1988**, 61, 2666. h) M. Mikuriya, I. Murase, E. Asato, S. Kida, *Chem. Lett.* **1989**, 497. i) A. Evers, R. Hancock, I. Murase, *Inorg. Chem.* **1986**, 25, 2160. j) E. Asato, S. Kida, I. Murase, *Inorg. Chem.* **1989**, 28, 800. k) G. Vuckovic, E. Asato, N. Matsumoto, S. Kida, *Inorg. Chim. Acta* **1990**, 171, 45. l) H. Harada, M. Koder, G. Vuckovic, N. Matsumoto, S. Kida, *Inorg. Chem.* **1991**, 30, 1190. m) L. H. Tan, M. R. Taylor, K. P. Wainwright, P. A. Duckworth, *J. Chem. Soc., Dalton Trans.* **1993**, 2921. n) R. Newell, A. Appel, D. L. DuBois, M. R. DuBois, *Inorg. Chem.* **2005**, 44, 365. o) A. M. Appel, R. Newell, D. L. DuBois, M. R. DuBois, *Inorg. Chem.* **2005**, 44, 3046.
- B. Bosnich, C. K. Poon, M. L. Tobe, *Inorg. Chem.* **1965**, 4, 1102.
- a) B. Chiswell, E. D. McKenzie, L. F. Lindoy, in *Comprehensive Coordination Chemistry*, ed. by G. Wilkinson, R. D. Gillard, J. A. McCleverty, Pergamon, Oxford, **1987**, Vol. 4, pp. 1–122. b) D. C. Weatherburn, S. Mandal, S. Mukhopadhyay, S. Bhaduri, L. F. Lindoy, in *Comprehensive Coordination Chemistry II*, ed. by J. A. McCleverty, T. J. Meyer, Elsevier, Amsterdam, **2004**, Vol. 5, pp. 1–125. c) *Manganese Redox Enzymes*, ed. by V. L. Pecoraro, VCH, New York, **1992**.
- a) G. W. Brudvig, R. H. Crabtree, *Prog. Inorg. Chem.* **1989**, 37, 99. b) R. Machanda, G. W. Brudvig, R. H. Crabtree, *Coord. Chem. Rev.* **1995**, 144, 1. c) A. J. Wu, J. E. Penner-Hahn, V. L. Pecoraro, *Chem. Rev.* **2004**, 104, 903.
- a) T. Matsushita, H. Kono, T. Shono, *Bull. Chem. Soc. Jpn.* **1981**, 54, 2646. b) T. Matsushita, Y. Hirata, T. Shono, *Bull. Chem. Soc. Jpn.* **1982**, 55, 108. c) T. Matsushita, T. Shono, *Polyhedron* **1983**, 2, 613. d) M. Fujiwara, T. Matsushita, T. Shono, *Polyhedron* **1985**, 4, 1895. e) H. Torayama, T. Nishide, H. Asada, M. Fujiwara, T. Matsushita, *Chem. Lett.* **1996**, 387. f) H. Torayama, H. Asada, M. Fujiwara, T. Matsushita, *Chem. Lett.* **1996**, 1067. g) H. Torayama, T. Nishide, H. Asada, M. Fujiwara, T. Matsushita, *Polyhedron* **1997**, 16, 3787. h) H. Torayama, T. Nishide, H. Asada, M. Fujiwara, T. Matsushita, *Polyhedron* **1998**, 17, 105. i) H. Torayama, H. Asada, M. Fujiwara, T. Matsushita, *Polyhedron* **1997**, 17, 3859.
- a) M. Mikuriya, Y. Hatano, E. Asato, *Bull. Chem. Soc. Jpn.* **1997**, 70, 2495. b) M. Mikuriya, H. Takebayashi, K. Matsunami, *Bull. Chem. Soc. Jpn.* **1994**, 67, 3128. c) M. Mikuriya, K. Matsunami, *Mater. Sci. (Poland)* **2005**, 23, 773. d) M. Mikuriya, R. Nukada, W. Tokii, Y. Hashimoto, T. Fujii, *Bull. Chem. Soc. Jpn.* **1996**, 69, 1573. e) M. Mikuriya, D. Jie, Y. Kakuta, T. Tokii, *Bull. Chem. Soc. Jpn.* **1993**, 66, 1132. f) M. Mikuriya, K. Nakadera, T. Tokii, *Inorg. Chim. Acta* **1992**, 194, 129. g) M. Mikuriya, H. Fukumoto, T. Kako, *Inorg. Chem. Commun.* **1998**, 1, 225. h) M. Mikuriya, T. Fujii, T. Tokii, A. Kawamori, *Bull. Chem. Soc. Jpn.* **1993**, 66, 1675. i) M. Mikuriya, K. Majima, Y. Yamato, *Chem. Lett.* **1992**, 1929. j) M. Mikuriya, Y. Yamato, T. Tokii, *Chem. Lett.* **1992**, 1571. k) M. Mikuriya, Y. Yamato, T. Tokii, *Bull. Chem. Soc. Jpn.* **1992**, 65, 1466. l) M. Mikuriya, Y. Yamato, T. Tokii, *Bull. Chem. Soc. Jpn.* **1992**, 65, 2624. m) M. Mikuriya, K. Nakadera, T. Kotera, T. Tokii, W. Mori, *Bull. Chem. Soc. Jpn.* **1995**, 68, 3077. n) M. Mikuriya, Y. Hashimoto, A. Kawamori, *Chem. Lett.* **1995**, 1095. o) C. Palopoli, B. Chansou, J.-P. Tuchagues, S. Signorella, *Inorg. Chem.* **2000**, 39, 1458.
- a) K. Shindo, Y. Mori, K. Motoda, H. Sakiyama, N. Matsumoto, H. Okawa, *Inorg. Chem.* **1992**, 31, 4987. b) H. Sakiyama, K. Tokuyama, Y. Matsumura, H. Okawa, *J. Chem. Soc., Dalton Trans.* **1993**, 2329.
- a) Z. Zhang, C. Brouca-Cabarrecq, C. Hemmert, F. Dahan, J.-P. Tuchagues, *J. Chem. Soc., Dalton Trans.* **1995**, 1453. b) S. Theil, R. Yerrande, R. Chikate, F. Dahan, A. Bousseksou, S. Padhye, J.-P. Tuchagues, *Inorg. Chem.* **1997**, 36, 6279. c) C. Palopoli, B. Chansou, J.-P. Tuchagues, S. Signorella, *Inorg. Chem.* **2000**, 39, 1458.
- a) A. Garcia-Deibe, M. R. Bermejo, A. Sousa, C. A. McAuliffe, P. McGlynn, P. T. Ndifon, R. G. Pritchard, *J. Chem. Soc., Dalton Trans.* **1993**, 1605. b) M. R. Bermejo, A. G. Deibe, M. Rey, J. Sanmartin, A. Sousa, N. Aurangzeb, C. E. Hulme, C. A. McAuliffe, R. G. Pritchard, M. Watkinson, M. Helliwell, *J. Chem. Soc., Dalton Trans.* **1994**, 1265. c) C. E. Hulme, M. Watkinson, M. Haynes, R. G. Pritchard, C. A. McAuliffe, N. Jaiboon, B. Beagley, A. Sousa, M. R. Bermejo, M. Fondo, *J. Chem. Soc., Dalton Trans.* **1997**, 1805. d) M. Watkinson, M.

- Fondo, M. R. Bermejo, A. Sousa, C. A. McAuliffe, R. G. Pritchard, N. Jaiboon, N. Aurangzeb, M. Naeem, *J. Chem. Soc., Dalton Trans.* **1999**, 31. e) M. R. Bermejo, M. Fondo, A. Garcia-Deibe, A. M. Gonzalez, A. Sousa, J. Sanmartin, C. A. McAuliffe, R. G. Pritchard, M. Watkinson, V. Lukov, *Inorg. Chim. Acta* **1999**, 293, 210.
- 12 a) M. Mikuriya, Y. Yamazaki, *Chem. Lett.* **1995**, 373. b) S. Wada, M. Mikuriya, in *Achievement in Coordination, Bioinorganic and Applied Inorganic Chemistry*, ed. by M. Melnik, J. Sima, M. Tatarko, Slovakia Technical University Press, Bratislava, **2007**, pp. 201–207.
- 13 *Molecular Magnetism*, ed. by O. Kahn, VCH Publishers, New York, **1993**, p. 3.
- 14 *SHELXTL-NT*, v. 5.10, Bruker AXS, Inc., Madison, WI, **1999**.
- 15 *Infrared and Raman Spectra of Inorganic and Coordination Compounds, Part B*, 5th ed., ed. by K. Nakamoto, Wiley Interscience, New York, **1997**.
- 16 Y. Shimura, M. Nakahara, *Kagaku Sosetsu* **1976**, 13, 13.
- 17 M. S. Shongwe, M. Mikuriya, R. Nukada, E. W. Ainscough, A. M. Brodie, J. M. Waters, *Inorg. Chim. Acta* **1999**, 290, 228.
- 18 F. Akhtar, M. G. B. Drew, *Acta Crystallogr., Sect. B* **1982**, 38, 612.
- 19 a) K. Wieghardt, U. Bossek, B. Nuber, J. Weiss, *Inorg. Chim. Acta* **1987**, 126, 39. b) K. Meyer, J. Bendix, N. Metzler-Nolte, T. Weyhermuller, K. Wieghardt, *J. Am. Chem. Soc.* **1998**, 120, 7260. c) J. C. Kim, A. J. Lough, *Bull. Korean Chem. Soc.* **1999**, 20, 1241. d) J. Limburg, J. S. Vrettos, R. H. Crabtree, G. W. Brudvig, J. C. de Paula, A. Hassan, A.-L. Barra, C. Duboc-Toia, M.-N. Collomb, *Inorg. Chem.* **2001**, 40, 1698.
- 20 Crystallographic data for  $7 \cdot 2\text{CHCl}_3$ :  $\text{C}_{64}\text{H}_{66}\text{Cl}_6\text{Mn}_2\text{N}_{14}\text{O}_4$ , FW: 1417.89, monoclinic, space group  $C2/c$ ,  $a = 28.283(10)$  Å,  $b = 16.057(6)$  Å,  $c = 18.875(7)$  Å,  $\beta = 131.536(6)^\circ$ ,  $V = 6416(4)$  Å<sup>3</sup>,  $Z = 4$ ,  $D_{\text{calcd}} = 1.47$  g cm<sup>-3</sup>,  $D_{\text{m}} = 1.45$  g cm<sup>-3</sup>, crystal size  $0.32 \times 0.08 \times 0.07$  mm<sup>3</sup>,  $\mu(\text{Mo K}\alpha) = 0.704$  mm<sup>-1</sup>,  $\theta$  range:  $1.59$ – $24.71^\circ$ , No. of reflections: 15546, No. of unique reflections: 5458,  $R1[I > 2\sigma(I)] = 0.1238$ ,  $wR2[I > 2\sigma(I)] = 0.2107$ , Goodness-of-fit on  $F^2 = 0.983$ .
- 21 A. Neves, S. M. D. Erthal, I. Vencato, A. S. Ceccato, Y. P. Mascarenhas, O. R. Nascimento, M. Horner, A. A. Batista, *Inorg. Chem.* **1992**, 31, 4749.
- 22 N. Torihara, M. Mikuriya, H. Okawa, S. Kida, *Bull. Chem. Soc. Jpn.* **1980**, 53, 1610.
- 23 D. V. Behere, S. Mitra, *Inorg. Chem.* **1980**, 19, 992.
- 24 C. J. O'Connor, *Prog. Inorg. Chem.* **1982**, 29, 203.
- 25 B. J. Kennedy, K. S. Murray, *Inorg. Chem.* **1985**, 24, 1552.
- 26 X. S. Tan, D. F. Xiang, W. X. Tang, M. Q. Chen, *Polyhedron* **1997**, 16, 1273.